Systematic trends in the electronic structure parameters of 4d transition metal oxides SrMO$_3$ (M = Zr, Mo, Ru, and Rh)

Y. S. Lee
Center for Strongly Correlated Materials Research, Seoul National University, Seoul 151-747, Korea

J. S. Lee and T. W. Noh
School of Physics and Research Center for Oxide Electronics, Seoul National University, Seoul 151-747, Korea

Douck Young Byun and Kwang Soo Yoo
Department of Materials Science and Engineering, University of Seoul, Seoul 130-743, Korea

K. Yamaura and E. Takayama-Muromachi
Superconducting Materials Center, National Institute for Materials Science, 1-1 Namiki, Tsukuba, Ibaraki 305-0044, Japan

(February 1, 2008)

We investigated the electronic structures of the perovskite-type 4d transition metal oxides SrMO$_3$ (M = Zr, Mo, Ru, and Rh) using their optical conductivity spectra $\sigma(\omega)$. The interband transitions in $\sigma(\omega)$ are assigned, and some important physical parameters, such as on-site Coulomb repulsion energy U, charge transfer energy Δ_{pd}, and crystal field splitting $10Dq$, are estimated. It is observed that Δ_{pd} and $10Dq$ decrease systematically with the increase in the atomic number of the 4d transition metal. Compared to the case of 3d transition metal oxides, the magnitudes of Δ_{pd} and $10Dq$ are larger, but those of U are smaller. These behaviors can be explained by the more extended nature of the orbitals in the 4d transition metal oxides.

PACS number; 78.20.-e, 78.30.-j, 78.66.-w

I. INTRODUCTION

There have been lots of investigations on 3d transition metal oxides (TMO), including cuprates and manganites, because they show a variety of interesting electric and magnetic properties.[1,2] These behaviors are closely related to the strong electron-electron (*el-el*) correlation, which originates from the localized 3d-orbitals. On the other hand, 4d TMO have attracted relatively less attention because it was thought that the *el-el* correlation effects should be small and insignificant due to their more extended d-orbitals. However, numerous intriguing properties, such as superconductivity,[3] non-Fermi liquid behavior,[4] pseudogap formation,[5] and metal-insulator transitions,[6–8] have been observed recently in the 4d TMO, especially ruthenates and molybdates. These observations have stimulated new attention to the 4d TMO.

Because 4d TMO are characterized by more extended orbitals than 3d TMO, it has been generally believed that electrons in the extended 4d-orbitals feel rather weak on-site Coulomb repulsion energy U and exchange energy J, and the 4d-orbitals hybridize more strongly with neighboring orbitals, e.g., O 2p-orbitals, than 3d-orbitals. Additional interactions, such as spin-orbit coupling, also become significant.[9] However, these qualitative ideas are not sufficient to understand the intriguing physical phenomena observed in some 4d TMO. In 3d TMO, systematic investigations on U and charge transfer energy Δ_{pd} provide a basis to elucidate origins of numerous intriguing properties.[2,10,11] Unfortunately, there have been few quantitative studies about the electronic structures of 4d TMO, except ruthenates,[6,12] which makes it difficult to understand their physical properties in more depth. Quantitative information on physical parameters related to the electronic structures of TMO will serve as a starting viewpoint in investigating various 4d TMO with a potential to discover other new intriguing phenomena. And, they will also allow us to make comparisons with the 3d TMO cases, which can provide us a better understanding of physics of both TMO.

Optical spectroscopy is known to be a powerful tool to analyze the electronic structures of TMO by probing the joint density of states between unoccupied and occupied states. In this paper, we report a systematic investigation on the electronic structures of the perovskite-type 4d SrMO$_3$ (M = Zr, Mo, Ru, and Rh) by measuring their optical conductivity spectra $\sigma(\omega)$. From these series with the same structure and valency state M^{4+}, one can investigate how the electronic structures change with M. As far as we know, our study is the first systematic effort to investigate wide range optical properties of the 4d SrMO$_3$ series. Based on proper electronic structure diagrams, the interband transitions observed in their $\sigma(\omega)$ are assigned properly. From this, we estimate im-

portant physical parameters, such as Δ_{pd}, U, and crystal field splitting energy $10Dq$, which show systematic trends with M. Compared with the $3d$ cases, the magnitudes of Δ_{pd} and $10Dq$ are larger and those of U are smaller in the $4d$ SrMO$_3$ compounds. These behaviors can be understood as the more extended character of the $4d$-orbitals than the $3d$-ones. From our observations, it is found that these $4d$ oxides belong to the Mott-Hubbard regime.

II. EXPERIMENTAL TECHNIQUES

Polycrystalline $SrZrO_3$, $SrMoO_3$, and $SrRhO_3$ were prepared using the solid state reaction technique. For the $SrZrO_3$ sample, $SrCO_3$ and ZrO_2 were used as raw materials. After calcining and grinding repeatedly, the resultant powders were pressed into a pellet under 200 MPa using cold isostatic pressing. The $SrZrO_3$ pellet was sintered at 1700 °C for 5 hours. For the $SrMoO_3$ sample, the fine and pure SrO_2, MoO_3, and Mo powders were mixed with a composition of $SrMoO_3$. The mixture of approximately 0.2 g was placed into a gold capsule and then compressed at 6 GPa in a high-pressure apparatus. The sample was heated at 1300 °C for 1 hour and quenched to room temperature at the elevated pressure. For the $SrRhO_3$ sample, a preparation procedure similar to that of the $SrMoO_3$ sample was used. The details of this procedure were published elsewhere.[13] The high pressure of sintering technique is effective to provide metastable Mo^{4+} and Rh^{4+} states.[14] From x-ray diffraction measurements, it was confirmed that all the samples have a single phase. From *dc* resistivity and magnetization measurements, it was also found that their electric and magnetic properties are consistent with the previous reports.[13,15]

Just before optical measurements, we polished the sample surfaces up to 0.3 μm. Then, we measured reflectivity spectra from 5 meV to 30 eV at room temperature. In the energy region between 5 meV and 0.6 eV, we used a conventional Fourier transform spectrophotometer. Between 0.5 eV and 6.0 eV, we used a grating spectrophotometer. And, in the deep ultraviolet region above 6.0 eV, we used synchrotron radiation from the normal incidence monochromator beam line at Pohang Accelerator Laboratory. After the optical measurements, thin gold films were evaporated onto the samples and used for making corrections for light scattering loss from the rough sample surfaces.[16]

In order to obtain $\sigma(\omega)$ from the measured reflectivity spectra, we performed the Kramers-Kronig (KK) analysis. It was known that the KK analysis for the highly anisotropic polycrystalline samples could provide incorrect $\sigma(\omega)$.[17] However, all of our $4d$ TMO have the slightly distorted perovskite structure and their optical constants should be nearly isotropic, so the KK analysis could be applied without any problem. For the analysis, the reflectivity below 5 meV was extrapolated with the Hagen-Rubens relation for the metallic samples and with a constant value for the insulating $SrZrO_3$ sample. For a high frequency region, the reflectivity value at 30 eV was used for reflectivities up to 40 eV, above which ω^{-4} dependence was assumed. To check the validity of our KK analysis, we independently determined $\sigma(\omega)$ using spectroscopic ellipsometry techniques in the photon energy range of 1.5 - 5.5 eV. The $\sigma(\omega)$ data from the spectroscopic ellipsometry agreed quite well with the results from the KK analysis.[16]

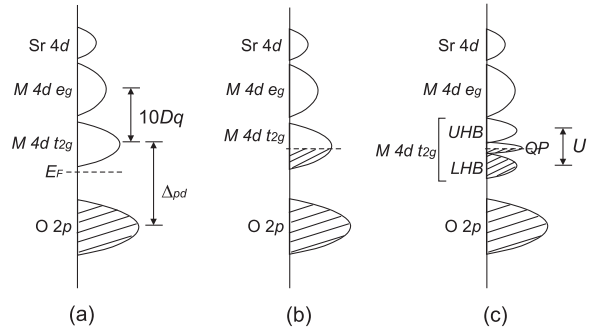

FIG. 1. Schematic diagrams of the electronic structures of perovskite-type 4d SrMO$_3$ with M = Zr, Mo, Ru, and Rh. (a) $SrZrO_3$ (a band insulator), (b) $SrMoO_3$ (a band metal), and (c) $SrRuO_3$ and $SrRhO_3$ (correlated metals). The dotted lines represent the Fermi level (E_F). In (c), the partially-filled t_{2g}-band is split into occupied lower Hubbard band (LHB) and unoccupied upper Hubbard band (UHB) by U in addition to the quasiparticle band (QP) located at E_F.

III. RESULTS AND DISCUSSIONS

A. Schematic diagrams of the electronic structures

Figure 1 shows schematic diagrams of the electronic structures of the perovskite-type SrMO$_3$ compounds, where the $4d$ transition metal M is either Zr, Mo, Ru, or Rh.[18] Figure 1(a) shows a typical diagram of electronic structure for a d^0-insulator. $SrZrO_3$ is known to be a $4d^0$-insulator with a bandgap between the O $2p$- and the Zr $4d$ t_{2g}-band.[1] The e_g-band has a higher energy level by $10Dq$ than the t_{2g}-band. Usually, the Sr $4d$-band is in a higher energy level than M $4d$-bands.[12] As the atomic number of M increases from Zr, extra $4d$ electrons start to fill the t_{2g}-band partially without any significant change in the overall feature of the band structure. Here, the details of the partially-filled t_{2g} orbitals can vary according to the *el-el* correlation. When the *el-el* correlation is quite weak, i.e., $4d$ bandwidth $W \gg U$, the partially-filled band induces a band metallic state, as shown in Fig. 1(b). Since $SrMoO_3$ is a $4d^2$-system and known to be a Pauli paramagnetic band metal,[15] its electronic structure should resemble Fig. 1(b). On the other hand, when the *el-el* correlation is quite large, i.e., $U \gg W$, the partially-filled band is split into two Hubbard bands by U, which induces a Mott insulator. In the

intermediate state between two extreme cases, there can occur correlated metals, whose band diagram is shown in Fig. 1(c). In the low-spin configuration, the quasiparticle band is located at E_F in addition to the Hubbard bands, and the e_g-band remains empty.[6,12] The electronic structure of $SrRuO_3$, a low-spin $4d^4$-system,[19] was investigated by earlier workers,[6,12] and known to follow Fig. 1(c). It was recently found that a $4d^5$-system $SrRhO_3$ is a paramagnetic correlated metal with the low-spin configuration.[13] Because the W of $SrRhO_3$ is narrower than that of $SrRuO_3$, the Hubbard bands induced by the *el-el* correlation are more dominant in $SrRhO_3$ than in $SrRuO_3$. So, the band diagram of $SrRhO_3$ can be also explained by Fig. 1(c).

According to the Fermi golden rule,[20] the *p-d* transitions such as O $2p \rightarrow M$ $4d$ t_{2g}, M $4d$ e_g, and Sr $4d$, should be distinct in $\sigma(\omega)$ of the $4d$ SrMO$_3$ systems. From such interband transitions, we can estimate some physical parameters; a charge transfer energy Δ_{pd} from the O $2p \rightarrow M$ $4d$ t_{2g} transition, and $10Dq$ from the energy difference between O $2p \rightarrow M$ $4d$ t_{2g} and M $4d$ e_g transitions. On the other hand, the U value should be estimated from the *d-d* transition between two Hubbard bands, which should be much weaker than the *p-d* transitions.

B. Assignment of interband transitions in the SrMO$_3$ compounds

Figure 2 shows $\sigma(\omega)$ of $SrZrO_3$ up to 20 eV. It is clearly shown that this insulating d^0-compound has a large optical gap of ~ 5.6 eV, consistent with the previous reports.[1] This value is larger by ~ 2 eV than the bandgap of $SrTiO_3$, i.e., 3.4 eV. Distinct interband transitions are observed around 8 eV and 12 eV. To our knowledge, there has been no band calculation report on this compound, so we assigned these interband transitions by referring to the band structure of $SrTiO_3$, which is a $3d^0$ insulator. The dotted line in Fig. 2 represents $\sigma(\omega)$ of $SrTiO_3$.[21] Its overall featurea are very similar to that of $SrZrO_3$, but with ~ 2.5 eV shift to lower energy. K. van Benthem *et al.* assigned the peaks around 5 eV and 9 eV of $SrTiO_3$ as O $2p \rightarrow$ Ti $3d$ t_{2g} and O $2p \rightarrow$ Ti $3d$ e_g transitions, respectively.[22] [They also claimed that the higher frequency peak should come from O $2p \rightarrow$ Ti $3d$ e_g and/or Sr $4d$.] Similarly, we can assign the peaks around 8 eV and 13 eV in $SrZrO_3$ as O $2p \rightarrow$ Zr $4d$ t_{2g} and O $2p \rightarrow$ Zr $4d$ e_g transitions, respectively. Note that these assignments are consistent with the energy diagram of a band insulator, shown in Fig. 1(a). By using the positions of the strong peaks, we can approximately estimate that $\Delta_{pd} \sim 8$ eV and $10Dq \sim 5$ eV in $SrZrO_3$, which are larger than the values for $SrTiO_3$ (i.e., $\Delta_{pd} \sim 5$ eV and $10Dq \sim 4$ eV).

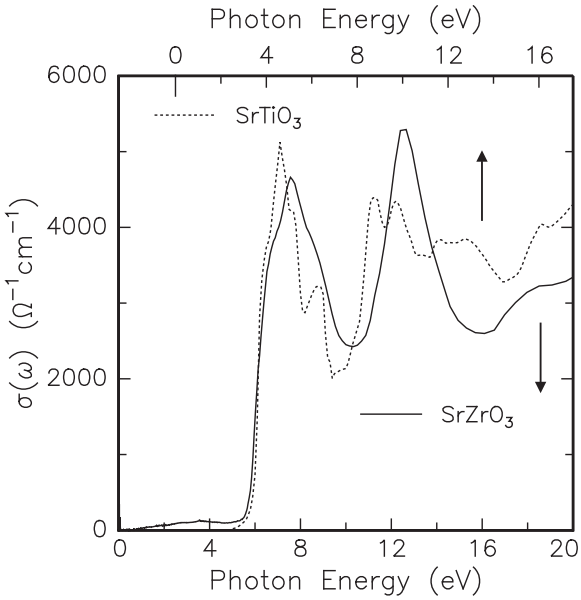

FIG. 2. Room temperature $\sigma(\omega)$ of $4d^0$ $SrZrO_3$ (the solid line) up to 20 eV. The $\sigma(\omega)$ of $3d^0$ $SrTiO_3$ (the dotted line), quoted from Ref. 21, is also displayed with a 2.5 eV shift to higher energy for comparison with $SrZrO_3$.

Figure 3 shows $\sigma(\omega)$ of the SrMO$_3$ series, with M = Zr, Mo, Ru, and Rh, up to 12 eV. The $\sigma(\omega)$ of $SrRuO_3$ is quoted from our previous paper.[6] The insulating $SrZrO_3$ has a relatively large optical gap. For other metallic compounds, $\sigma(\omega)$ below 1.0 eV have zero-frequency spectral weights, which decrease with the increasing atomic number of M. The coherent mode of the band metallic $SrMoO_3$ can be fitted well by the Drude model with a plasma frequency of ~ 2.8 eV and a scattering rate of ~ 0.3 eV. For other correlated metallic $SrRuO_3$ and $SrRhO_3$, the low frequency $\sigma(\omega)$ decreases more slowly than the $1/\omega^2$-dependence which is predicted by the Drude model. This behavior, which have often been observed in many correlated metals,[2] indicates that the incoherent character in the mid-infrared region might be rather strong.[4]

The observed peaks of the SrMO$_3$ compounds can be assigned according to their electronic structures shown in Fig. 1. It is noted that, according to the Fermi golden rule, the *p-d* transition should be dominant in $\sigma(\omega)$. The assignments for the $SrZrO_3$ peaks were already given. For $SrMoO_3$, the 5.0 eV and 8.5 eV peaks are observed clearly, as shown in Fig. 3(b). These two peaks can be assigned as O $2p \rightarrow$ Mo $4d$ t_{2g} and O $2p \rightarrow$ Mo $4d$ e_g transitions. For $SrRuO_3$, the 3.0 eV, 6.0 eV, and 10 eV peaks shown in Fig. 3(c) can be assigned as O $2p \rightarrow$ Ru $4d$ t_{2g}, O $2p \rightarrow$ Ru $4d$ e_g, and O $2p \rightarrow$ Sr $4d$ transitions, respectively, according to our previous report.[6] Note that the *d-d* transition between the lower and the upper Hubbard bands is located around 1.7 eV, but too weak to be clearly seen in this compound.[6]

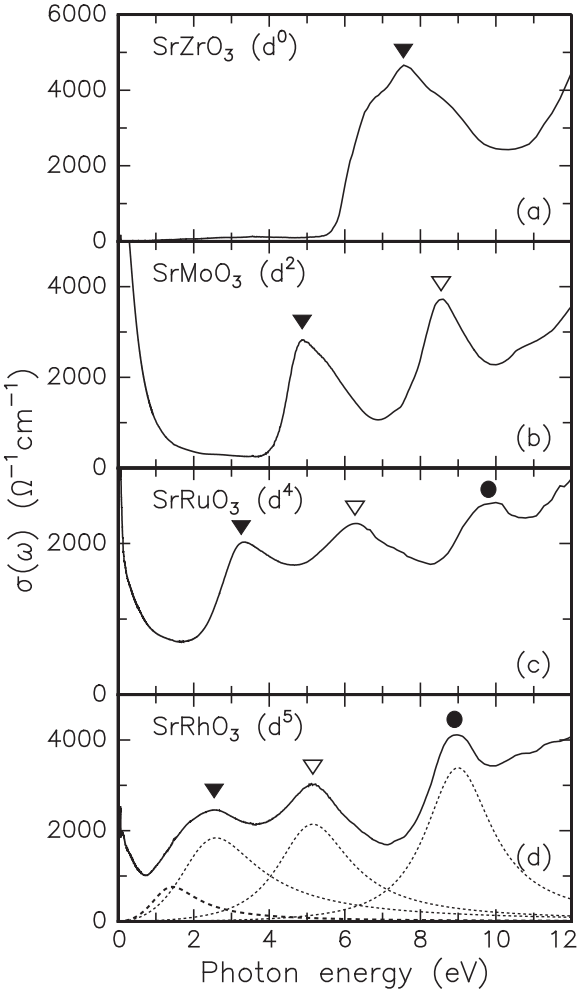

FIG. 3. Room temperature $\sigma(\omega)$ of the 4d $SrMO_3$ series. (a) $SrZrO_3$ (d^0), (b) $SrMoO_3$ (d^2), (c) $SrRuO_3$ (d^4), and (d) $SrRhO_3$ (d^5) up to 12 eV. The solid triangles, the open triangles, and the solid circles represent the positions of the O $2p \rightarrow M$ $4d$ t_{2g}, the O $2p \rightarrow M$ $4d$ e_g, and the O $2p \rightarrow$ Sr $4d$ transitions, respectively. In (d), the dotted lines represent the fitting results on the $\sigma(\omega)$ of $SrRhO_3$ with Lorentz oscillators.

The interband transitions in $SrRhO_3$ can be similarly assigned for the case of $SrRuO_3$. However, the lowest interband transition near 2.5 eV is quite asymmetric with a broad tail in the low energy region, compared with the corresponding one in $SrRuO_3$. From the electronic structure shown in Fig. 1(c), we fitted this peak with two Lorentz oscillators, where a lower energy peak with a relatively small strength can be assigned as the d-d transition between the Hubbard bands. The fitting results are represented by the dotted lines in Fig. 3(d). From this fitting, the 1.6 eV, 2.6 eV, 5.2 eV, and 9.0 eV peaks in $SrRhO_3$ can be assigned as the d-d transition between Hubbard bands, O $2p \rightarrow$ Rh $4d$ t_{2g}, O $2p \rightarrow$ Rh $4d$ e_g, and O $2p \rightarrow$ Sr $4d$ transitions, respectively. The relatively stronger d-d transition in $SrRhO_3$ indicates that the carriers in this compound should be more correlated than those in $SrRuO_3$.

It is interesting to observe systematic trends in the interband transitions of the $SrMO_3$ series. As it goes from $SrZrO_3$ to $SrRhO_3$, all of the p-d transitions shift to lower energies. In the photon energy region up to 12 eV, only the O $2p \rightarrow M$ $4d$ t_{2g} transition is observed in $SrZrO_3$, but the O $2p \rightarrow M$ $4d$ e_g transition is additionally observed in $SrMoO_3$. And, in $SrRuO_3$ and $SrRhO_3$, the O $2p \rightarrow$ Sr $4d$ transition as well as the O $2p \rightarrow M$ $4d$ transition are observed. Note that as the atomic number of M increases, the O $2p \rightarrow M$ $4d$ transitions shift to the lower energy side. In addition, the peak interval between the O $2p \rightarrow M$ $4d$ t_{2g} and the O $2p \rightarrow M$ $4d$ e_g transitions decreases. These interesting trends in peak positions should be originated from the systematic changes of Δ_{pd} and $10Dq$.

C. Systematic trends in Δ_{pd} and $10Dq$

Figure 4(a) shows a systematic trend in the Δ_{pd} values, which are estimated from the position of the O $2p \rightarrow M$ $4d$ t_{2g} transition. As the atomic number increases, Δ_{pd} decreases. According to J. B. Torrance *et al.*'s work with the ionic model,[23] the change of Δ_{pd} with the atomic number of a transition metal is attributed mainly to the change in electronegativity (or ionization energy) of a transition metal; as the electronegativity of a transition metal becomes larger, the Δ_{pd} decreases. So, the decrease of Δ_{pd} in $4d$ $SrMO_3$ can be explained by the larger electronegativity of M with its atomic number increasing.

Figure 4(b) shows a systematic trend in the $10Dq$ values, which are estimated from the peak position difference between the O $2p \rightarrow M$ $4d$ t_{2g} and the O $2p \rightarrow M$ $4d$ e_g transitions. The $10Dq$ of $SrZrO_3$ is approximately estimated to be ~ 5 eV, as shown in Fig. 2. The $10Dq$ value of $SrMoO_3$, ~ 3.8 eV, is comparable to that in Mo $4d$-bands of double perovskite Sr_2FeMoO_6, ~ 4 eV, from x-ray absorption spectroscopy.[24] $SrRhO_3$ is estimated to have $10Dq \sim 2.6$ eV, a little smaller than that of $SrRuO_3$, i.e., 3 eV. It is noted that the $10Dq$ decreases with the increasing atomic number of M. It is generally accepted that, as the overlap (or covalency) between the O $2p$- and the d-orbital becomes stronger, $10Dq$ becomes larger. So, the decrease of the $10Dq$ in the $4d$ $SrMO_3$ series can be understood as the shrinking of the d-orbitals, and the resultant weakening of the covalency between the M $4d$- and the O $2p$-orbitals with the increasing atomic number. For a quantitative analysis, we estimate the covalency strength as the p-d matrix element with the σ-bonding, $V_{pd\sigma} \propto d_r^{1.5}/d_{M-O}^{3.5}$, suggested by W. A. Harrison.[25,26] Here, d_r and d_{M-O} are the radial size of the d-orbital[25] and the distance between the M and the O ions, respectively. As shown in the inset of Fig. 4(b), the value of $d_r^{1.5}/d_{M-O}^{3.5}$ in the $4d$ compounds decreases with increasing atomic number of M, consistent with the decrease of $10Dq$. This suggests that the p-d covalency should play

a crucial role in determining the $10Dq$ value.[27]

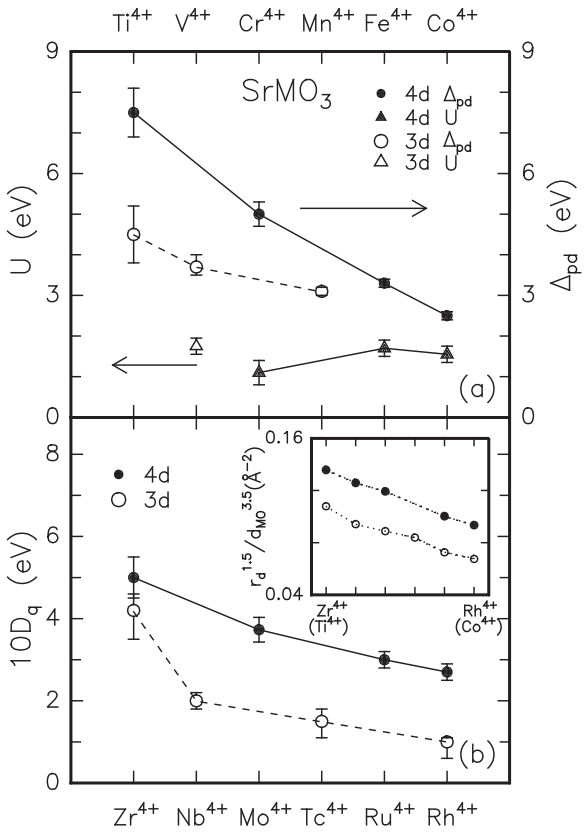

FIG. 4. (a) Charge transfer energy Δ_{pd} and on-site Coulomb repulsion energy U, and (b) crystal field splitting energy $10Dq$ in $4d$ SrMO$_3$ with M = Zr, Mo, Ru, and Rh (solid symbols) and $3d$ SrM'O$_3$ with M' = Ti,[22] V,[28] Mn,[29,33] and Co[31] (open symbols). Note that these parameters are estimated from the optical measurements only, except the $10Dq$ value of SrCoO$_3$.[31] In the inset of Fig. 4(b), the values of $d_r^{1.5}/d_{M-O}^{3.5}$ are estimated in the $3d$ and the $4d$ oxides. The values of d_r are used from Ref. 25. [We also estimated d_r from the ionic size of M^{4+} (M'^{4+}). The results show the similar trends, except the case of SrFeO$_3$.] The d_{M-O} of the $3d$ compounds are used from Ref. 23. For the $4d$ oxides, because detailed structural analyses have not been done, we used the values of d_{M-O} as half of the pseudo-cubic lattice constants, which are obtained from x-ray diffraction measurements. The pseudo-cubic lattice constants a of SrZrO$_3$, SrMoO$_3$, SrRuO$_3$, and SrRhO$_3$ are 4.11 Å, 3.97 Å, 3.94 Å, and 3.92 Å, respectively. The a value of 4.02 Å is used for SrNbO$_3$ [H. Hannerz *et al.*, J. Solid State Chem. **147**, 421 (1999)].

D. Comparison with 3d transition metal oxides

We also display the reported results on some $3d$ SrM'O$_3$ with a $3d$ transition metal M'= Ti, V, Mn, and Co in Fig. 4. Most of the displayed results were determined from $\sigma(\omega)$ in the same way as was adopted in this paper. Note that we include only the optical results except for the $10Dq$ value of SrCoO$_3$. In Fig. 4(a), the values of Δ_{pd} in the $3d$ SrM'O$_3$ series are displayed as the open circles.[22,28,29] Similar to the case of the $4d$ TMO, Δ_{pd} decreases as the atomic number of M' increases. [While there are no optical reports on metallic SrFeO$_3$ and SrCoO$_3$, photoelectron spectroscopy (PES) results claimed that their Δ_{pd} values be nearly zero.[30,31]] However, the magnitudes of Δ_{pd} in $4d$ SrMO$_3$ are relatively larger than those of $3d$ SrM'O$_3$ with the same electron occupancy in d-orbitals. As mentioned earlier, the systematic change of Δ_{pd} is attributed to the change in electronegativity. The larger Δ_{pd} values in the $4d$ SrMO$_3$ series than those in the $3d$ SrM'O$_3$ series can be also explained by the smaller electronegativity for $4d$ transition metals.[32]

In Fig. 4(b), the reported values of $10Dq$ in the $3d$ SrM'O$_3$ series are plotted as the open circles.[22,28,31,33] The general trend of $10Dq$ in the $3d$ series is also similar to that in the $4d$ series. It is interesting to see that the $10Dq$ of $4d$ SrMO$_3$ is larger than that of $3d$ SrM'O$_3$. This behavior is consistent with the larger values of $d_r^{1.5}/d_{M-O}^{3.5}$ in $4d$ SrMO$_3$ than those in $3d$ SrM'O$_3$, shown in the inset. It is evident that the more extended $4d$-orbitals induce stronger p-d covalency, which causes the $10Dq$ values of the $4d$ oxides to be larger than those of the $3d$ oxides.

While the high-spin configuration is more prevalent in $3d$ TMO, the low-spin configuration can be more easily found in $4d$ SrMO$_3$. This behavior should be closely related to the relatively larger $10Dq$ values in the $4d$ SrMO$_3$ series. The spin-configuration in TMO is determined according to the relative magnitude of $10Dq$ and J: a high-spin configuration for $10Dq < J$, and a low-spin configuration for $10Dq > J$. It is known that some $3d$ TMO, such as Mn- and Fe-oxides, have the high-spin configuration. For example, the values of $10Dq$ and J in Mn-oxides are estimated to be 1.1 $\sim$ 1.8 eV[33] and $\sim$ 3 eV[29], respectively. On the other hand, $4d$ TMO favor the low-spin configuration with the relatively larger $10Dq$ and smaller J due to the more extended $4d$-orbitals. For Ru-oxides, the values of $10Dq$ and J are estimated to be 3 eV and 0.5 $\sim$ 0.6 eV,[12,34] respectively. Although there is no report about J in SrRhO$_3$, the large $10Dq$ value of $\sim$ 2.6 eV strongly suggests that this compound should have the low-spin configuration. Because the Rh $4d$-orbitals become more extended in the Rh^{3+} state than in the Rh^{4+} state, an insulating $4d^6$ LaRhO$_3$ material with a Ru^{3+} state is very likely to be a band-insulator which has fully-occupied t_{2g} orbitals in the low-spin configuration.

In the $3d$ TMO, the character of the low energy charge excitations has been investigated intensively.[2,10,11] According to Zaanen, Sawatzky, and Allen's picture,[35] the charge excitation should be the d-d transition between the Hubbard bands, if $U < \Delta_{pd}$. This is classified as the Mott-Hubbard regime. If $U > \Delta_{pd}$, the low energy excitation should be a p-d transition, and this regime is classified as the charge transfer regime. While the early $3d$ TMO are classified to be in the Mott-Hubbard regime ($U < \Delta_{pd}$), the late $3d$ TMO mainly fall in the

charge-transfer regime ($U > \Delta_{pd}$), implying some kind of crossover between the two regimes.[2,10] This behavior is related to the increase of U and the decrease of Δ_{pd} as the atomic number of a transition metal increases.

To find the character of the low energy charge excitation in the 4*d* SrMO$_3$ series, we estimated the values of U from the position of the *d*-*d* transition between the Hubbard bands in $\sigma(\omega)$. The values of U for SrMoO$_3$ and SrRuO$_3$ are estimated from the previous studies.[6,36] Note that the U value obtained from $\sigma(\omega)$ is usually somewhat smaller than that measured from PES, due to the exciton effects, but its difference between optical spectroscopy and PES is usually less than 1.0 eV.

In Fig. 4(a), the values of U for the 4*d* SrMO$_3$ series are plotted as solid triangles. It appears that the magnitude of U in 4*d* SrMO$_3$ is relatively smaller than that in 3*d* SrM'O$_3$. As shown in Fig. 4(a), the value of $U \sim 2$ eV in SrVO$_3$ (d^2)[28] is comparable to those of SrRuO$_3$ and SrRhO$_3$, 1.6 - 1.7 eV. Generally, the U value increases as the size of the *d*-orbitals decreases. Because the *d*-orbital shrinks as the the atomic number increases, the late 3*d* SrM'O$_3$, such as SrFeO$_3$ (d^4) and SrCoO$_3$ (d^5), are expected to have larger U than the early 3*d* SrVO$_3$, as has been confirmed by many PES studies.[2,11] From this, it is clear that the U value of SrRuO$_3$ and SrRhO$_3$ should be smaller than those of SrFeO$_3$ and SrCoO$_3$.[37] So, we can say safely that 4*d* SrMO$_3$ have smaller U than 3*d* SrM'O$_3$, which is quite natural due to the more extended nature of the 4*d*-orbitals.

The larger value of Δ_{pd} than U indicates that all of the 4*d* SrMO$_3$ compounds investigated in this study should belong to the Mott-Hubbard regime. From our studies on SrRuO$_3$ and SrRhO$_3$, the magnitude of Δ_{pd}, 2.6 - 3.0 eV, is larger than that of U, 1.6 - 1.7 eV, which indicates that even these compounds belong to the Mott-Hubbard regime. This implies that these 4*d* TMO can be used for investigating the Mott-Hubbard transition with the *el*-*el* correlation. Indeed, the importance of the *el*-*el* correlation has been observed in ruthenates and molybdates,[6,7] This was rather surprising, since it was thought that the *el*-*el* correlation effects should be insignificant in 4*d* TMO due to the extended nature of the 4*d*-orbitals. And, due to the small value of U, the multiplicity of the 4*d* orbitals might play important roles in physical properties of some 4*d* TMO.[38] It is highly desirable to reinvestigate physical properties of some 4*d* TMO in view of the correlation effects.

IV. SUMMARY

We reported quantitative studies on physical parameters such as charge transfer energy Δ_{pd}, on-site Coulomb repulsion energy U, and crystal field splitting energy $10Dq$ of the perovskite-type of various 4*d* SrMO$_3$ (M = Zr, Mo, Ru, and Rh) by optical conductivity analyses. While the systematic changes of these parameters with the transition metal are similar to those for the case of 3*d* transition metal oxides, their magnitudes are different; the Δ_{pd} and the $10Dq$ values are relatively larger, while the U value is relatively smaller. These behaviors are explained by the more extended character in 4*d*-orbitals than in 3*d*-orbitals, which distinguishes the physical properties of the 4*d* compounds from those of the 3*d* ones. The relatively larger $10Dq$ is closely related to the low-spin configuration in 4*d* SrMO$_3$. Due to the relatively smaller U and larger Δ_{pd}, it is very likely that most 4*d* transition metal oxides lie in the Mott-Hubbard regime. Although their U values are relatively small, some intriguing physical phenomena with the correlation effects could occur in 4*d* transition metal oxides.

ACKNOWLEDGMENTS

We would like to thank Jaejun Yu, S.-J. Oh, and S. D. Bu at SNU and D. Y. Jung at SKKU for useful discussions. This work was supported by the Ministry of Science and Technology through the Creative Research Initiative program, and by KOSEF through the Center for Strongly Correlated Materials Research. The experiments at PLS were supported by MOST and POSCO.

[1] P. A. Cox, *Transition metal oxides* (Clanrendon press, Oxford, 1992).
[2] M. Imada, A. Fujimori, and Y. Tokura, Rev. Mod. Phys. **70**, 1039 (1998).
[3] Y. Maeno, H. Hashimoto, K. Yoshida, S. Nishizaki, T. Fujita, J. G. Bednorz, and F. Lichtenberg, Nature **372**, 532 (1995).
[4] P. Kostic, Y. Okada, N. C. Collins, Z. Schlesinger, J. W. Reiner, L. Klein, A. Kapitulnik, T. H. Geballe, and M. R. Beasley, Phys. Rev. Lett. **81**, 2498 (1998). Y. S. Lee *et al.*, cond-mat/0205526.
[5] Y. S. Lee *et al.*, Europhys. Lett. 55, 280 (2001). Y. S. Lee *et al.*, Phys. Rev. B **64**, 165109 (2001).
[6] J. S. Lee, Y. S. Lee, T. W. Noh, K. Char, Jonghyuk Park, S.-J. Oh, J.-H. Park, C. B. Eom, T. Takeda, and R. Kanno, Phys. Rev. B **64**, 245107 (2001).
[7] T. Katsufuji, H. Y. Hwang, and S.-W, Cheong, Phys. Rev. Lett. **84**, 1998 (2000).
[8] J. S. Lee, Y. S. Lee, K. W. Kim, T. W. Noh, J. Yu, T. Takeda, and R. Kanno, Phys. Rev. B **64**, 165108 (2001).
[9] T. Mizokawa, L. H. Tjeng, G. A. Sawatzky, G. Ghiringhelli, O. Tjernberg, N. B. Brooks, H. Fukazawa, S. Kakatsuji, and Y. Maeno, Phys. Rev. Lett. **87**, 077202 (2001).
[10] T. Arima, Y. Tokura, and J. B. Torrance, Phys. Rev. B **48**, 17006 (1993).
[11] A. E. Bocquet, T. Mizokawa, K. Morikawa, A. Fujimori, S. R. Barman, K. Maiki, D. D. Sarma, Y. Tokura, and M. Onoda, Phys. Rev. B **53**, 1161 (1996).

[12] J. Okamoto, T. Mizokawa, A. Fujimori, I. Hase, M. Nohara, H. Takagi, Y. Takeda, and M. Takano, Phys. Rev. B **60**, 2281 (1999).
[13] K. Yamaura and E. Takayama-Muromachi, Phys. Rev. B **64**, 224424 (2001).
[14] S. Yamaoka, M. Akaishi, H. Kanda, T. Osawa, T. Taniguchi, H. Sei, and O. Fukunaga, J. High Pressure Inst. Jpn. **30**, 249, (1992).
[15] R. Agarwal, Z. Singh, and Venugopal, J. Alloys Compounds **282**, 231 (1999).
[16] H. J. Lee, J. H. Jung, Y. S. Lee, J. S. Ahn, T. W. Noh, K. H. Kim, and S.-W. Cheong, Phys. Rev. B **60**, 5251 (1999).
[17] J. Orenstein and D. H. Rapkine, Phys. Rev. Lett. **60**, 968 (1988).
[18] $SrNbO_3$, which has barely been synthesized, is known to be a Pauli paramagnetic band metal, similar to $SrMoO_3$ [H. Hannerz *et al.*, J. Solid State Chem. **147**, 421 (1999)]. $SrTcO_3$ has not been synthesized. And, $SrPdO_3$ is a non-perovskite material.
[19] P. B. Allen, H. Berger, O. Chauvet, L. Forro, T. Jarlborg, A. Junod, B. Revaz, and G. Santi, Phys. Rev. B **53**, 4393 (1996).
[20] F. Wooten, *Optical Properties of Solids* (Academic press, New York and London, 1972).
[21] F. Gervais, *Handbook of optical constants of Solid II*, edited by Edward D. Palik (Academic press, San diego, 1991).
[22] K. van Benthem, C. Elsässer, and R. H. French, J. Appl. Phys. **90**, 6156 (2001).
[23] J. B. Torrance, P. Lacorre, C. Asavaroengchai, and R. M. Metzger, Phyica C **182**, 351 (1991).
[24] J. H. Jung *et al.*, (unpublished).
[25] W. A. Harrison, *Electronic structure and Physical Properties of Solids* (Freeman, San Francisco, 1980).
[26] The p-d matrix element with the σ-bonding $V_{pd\sigma} = \eta_{pd\sigma} \cdot d_r^{1.5}/d_{M(M')-O}^{3.5}$, and the p-d matrix element with the π-bonding $V_{pd\pi} = \eta_{pd\pi} \cdot d_r^{1.5}/d_{M(M')-O}^{3.5}$. Here, $\eta_{pd\sigma} = (-2.17)\eta_{pd\pi}$,[25] and represents the anisotropic covalency strength of the O $2p$ orbitals with the t_{2g}- and the e_g-orbitals. So, the quantity, $d_r^{1.5}/d_{M(M')-O}^{3.5}$ can be a parameter related to the $10Dq$ between the t_{2g}- and the e_g-orbitals.
[27] S. Sugano and R. G. Shulman, Phys. Rev. **130**, 517 (1963).
[28] H. F. Pen, M. Abbate, A. Fujimori, Y. Tokura, H. Eisaki, S. Uchida, and G. A. Sawatzky, Phys. Rev. B **59**, 7422 (1999). M. J. Rozenberg, G. Kotliar, H. Kajueter, G. A. Thomas, D. H. Rapkine, J. M. Honig, and P. Metcalf, Phys. Rev. Lett. **75**, 105 (1995).
[29] J. H. Jung, K. H. Kim, D. J. Eom, T. W. Noh, E. J. Choi, J. Yu, Y. S. Kwon, and Y. Chung, Phys. Rev. B **55**, 15489 (1997).
[30] A. E. Bocquet, A. Fujimori, T. Mizokawa, T. Saitoh, H. Namatame, S. Suga, N. Kimizuka, Y. Takeda, and M. Takano, Phys. Rev. B **45**, 1561 (1992).
[31] R. H. Potze, G. A. Sawatzky, and M. Abbate, Phys. Rev. B **51**, 11501 (1995).
[32] As the Madelung potential difference between a transition metal and O sites, ΔV_M increases, so does Δ_{pd}. Because the lattice constants of $4d$ SMO_3 are larger than those of $3d$ $SM'O_3$, ΔV_M is expected to be smaller in $4d$ SMO_3 than in $3d$ $SM'O_3$. So, the contribution of ΔV_M cannot explain the larger Δ_{pd} of $4d$ SMO_3 than those of $3d$ $SM'O_3$.
[33] Y. Moritomo, T. Arima, and Y. Tokura, J. Phys. Soc. J. **64**, 4117 (1995). K. Takenaka, Y. Sawaki, R. Shiozaki, and S. Sugai, Phys. Rev. B **62**, 13 864 (2000).
[34] D. Singh, J. Appl. Phys. **79**, 4818 (1996).
[35] J. Zarren, G. A. Sawaksy, and J. W. Allen, Phys. Rev. Lett. **55**, 418 (1985).
[36] The U value of $SrMoO_3$ is regarded as that of a Mott insulator $Y_2Mo_2O_7$ with a Mo^{4+} state [Y. Taguchi, K. Ohgushi, and Y. Tokura, Phys. Rev. B **65**, 115102 (2002)].
[37] From PES results, the U value of $SrRuO_3$ is $\sim$ 3 eV,[12] while that of $SrFeO_3$ is $\sim$ 7.8 eV.[30]
[38] J.-H. Park, L. H. Tjeng, A. Tanaka, J. W. Allen, C. T. Chen, P. Metcalf, J. M. Honig, F. M. F. de Croot, and G. A. Sawatzky, Phys. Rev. B 61, 11 506 (2001) and the references therein.